OSTEOBLAST RESPONSE TO ZINC-DOPED SINTERED β-TRICALCIUM PHOSPHATE

Sahil Jalota, Sarit B. Bhaduri, and A. Cuneyt Tas
School of Materials Science and Engineering
Clemson University
Clemson, SC 29634

ABSTRACT

Sintered β-tricalcium phosphate (β-TCP, β-$Ca_3(PO_4)_2$) and Zn-doped (600, 4100, and 10100 ppm) β-TCP samples were prepared by using an aqueous chemical synthesis technique, followed by the calcination of pressed powders at 1000°C in air. Precursor powders of the synthesis process were Ca-deficient nanoapatites (i.e., Ca/P molar ratio varying from 1.49 to 1.51) with rod-like but agglomerated particles of 50 nm length and 20 nm thickness. In vitro culture tests performed by mouse osteoblast-like cells showed that β-TCP doped with 4100 ppm Zn had the highest cell viability and alkaline phosphatase (ALP) activity values over a range of 0 to 1 wt% Zn. The sample surface roughness, measured by non-contact profilometry, was also found to have an effect on the Live/Dead cell counts, and the highest cell viability recorded in this study corresponded to the surfaces with the least roughness.

INTRODUCTION

The most commonly used synthetic bone implant materials are Ca-hydroxyapatite (HA, $Ca_{10}(PO_4)_6(OH)_2$) and β-tricalcium phosphate (β-TCP, β-$Ca_3(PO_4)_2$).[1] These materials possess exceptionally good tissue compatibility and bond directly to bone without an intermediary layer of fibrous tissue.[2] Calcium phosphate (CaP)-based synthetic implants provide, *in vivo*, calcium and phosphate ions to the implant-host bone interface as soon as their resorption starts.[2] The inorganic part of bone is made up of a defective and rather complex substance (also doped with several mono- or divalent cations (Na, K, Mg, Zn, Fe, etc.) as well as with carbonate ions) with a generic formula of $Ca_{8.3}(PO_4)_{4.3}(HPO_4, CO_3)_{1.7}(OH, CO_3)_{0.3}$.[3] Divalent cations, which partially substitute the calcium and phosphate sites in these implant structures, seem to play an important role in the competition between HA and β-TCP.[4] However, β- TCP has an advantage over HA in the sense that β-TCP dissolves and resorbs faster than HA. It was shown that the dissolution rate of β-TCP (i.e., 1.26×10^{-4} mol/m^{-2} min^{-1}) in an aqueous solution at a pH of about 6 was about 89 times greater than that of carbonated apatite (1.42×10^{-6} mol/m^{-2} min^{-1}).[5] As an implant the higher dissolution rate of β-TCP may result in premature loss of mechanical strength. It was shown that when the TCP structure was stabilized, the dissolution rate will decrease,[6, 7] providing better mechanical properties. This stability in structure can be achieved by substituting the larger Ca^{2+} (0.099 nm) ions with smaller divalent cations, such as Zn^{2+} (0.074 nm)[6, 8] or Mg^{2+} (0.072 nm) ions.[7] It was reported that the solubility activity product (K_{sp}) of single phase pure β-TCP is 2.51×10^{-30} [9, 10] and that of Zn-doped TCP decreases by 52-92% in increasing the Zn-level up to 630 ppm.[6] Stabilization of the β-TCP structure was quite evident from the fact that there was an increase in the transformation temperature of Zn-doped β-TCP to α-TCP.[11] As a result, Zn-doped β-TCP can be sintered at higher temperatures without its conversion to α-TCP.

Zinc is an important growth factor, as deficiency of zinc can adversely affect growth in many animal species and in humans.[12] The deficiency of zinc can also cause severe disorders as poor appetite, mental lethargy, delayed wound healing, growth retardation, delayed puberty in adolescents, and rough skin.[12] The supplementation of zinc can help reduce the susceptibility to diseases like diarrhea, pneumonia, respiratory infections, and poor immune system.[13] Zinc is essential for maintaining biologically good health in humans. In humans, zinc is present as a trace element in the bones, teeth, hair, skin, testes, liver, and muscles. Zinc also promotes synthesis of deoxyribonucleic acid (DNA) and ribonucleic acid (RNA). Zinc has a stimulatory effect on bone formation and mineralization, both in vivo and in vitro.[14-16] The presence of zinc is known to increase the protein synthesis,[17-19] to activate the aminoacyl-tRNA synthase,[19, 20] to enhance albumin synthesis,[18] and to increase ALP activity.[15] It should be noted here that a protein called osterix (i.e., zinc finger-containing transcription factor) is needed for osteoblast differentiation.[21] While it was shown that the presence of zinc led to an increase in osteoblast activity, it was also shown that zinc's deficiency led to bone growth retardation,[22,23] postmenopausal osteoporosis,[24] and programmed cell apoptosis (in mice).[25] However, there comes a limitation in the amount of zinc which can increase the activity of osteoblast cells, as high concentrations of zinc may also have a cytotoxic effect on cells.[26] Therefore, in this study we placed the significance on finding the appropriate zinc concentration needed for enhanced osteoblast cell proliferation, response and growth.

The synthesis of zinc containing calcium phosphates has been initialized by Bigi *et al.*[4] and Fuierer *et al.*[27] Bigi *et al.* synthesized Zn-doped β-TCP by physically mixing the in-house synthesized single phase β-TCP with α-$Zn_3(PO_4)_2$, followed by calcining the mixture at 1000°C for 15 hours.[8] In the aforementioned studies no ICP data were reported which would have been of great help in determining any vaporization of Zn occurring while heating the samples at such high temperatures for prolonged times. Another important contribution to the synthesis of Zn-doped β-TCP was made by LeGeros *et al.*,[28,29] where the precursor powders were formed by wet chemical methods. However, until now the research group of Ito *et al.*[6, 30-42] have been the most important contributor to the synthesis of Zn-doped β-TCP (and other calcium phosphates), as well as their *in vitro* and *in vivo* evaluation. Ito *et al.* have shown the positive stimulatory effects of Zn on *in vivo* bone formation. The most preferred route of the Ito group in synthesizing the Zn-doped β-TCP was a two-step procedure.[31] Briefly, they first prepared a 10 mol% Zn-doped β-TCP and then mixed it in an alumina mortar with appropriate amounts of commercially available pure β-TCP to obtain the desired amount of Zn-doping. 10 mol% Zn-doped β-TCP was synthesized by mixing a suspension of calcium hydroxide (synthesized in-house by forming calcium oxide from calcium carbonate by heating the latter at 1000ºC for 3 h and then dissolving the former in water) with zinc nitrate hexahydrate and a phosphoric acid solutions.[31] The precipitates were then filtered and calcined at 850ºC for 1 h.[31] The authors also reported the presence of a secondary phase of $CaZn_2(PO_4)_2$ while attempting to synthesize TCP containing zinc more than 12 mol%. After mixing 10 mol% Zn-doped β-TCP with pure β-TCP, various samples were reported to be synthesized, such as containing 0.28, 2.56, 5.0, 7.47, and 10.5% Zn.[31]

We realized that the lower end of Zn-doping range was not fully explored. Therefore, in this study we tried to explore the range of Zn-doping from pure β-TCP to 1.0 wt% Zn-doped β-TCP. We synthesized the powders by using an aqueous chemical route which used $Ca(NO_3)_2{\cdot}4H_2O$, $NH_4H_2PO_4$, and $Zn(NO_3)_2{\cdot}6H_2O$ as the starting chemicals. Precursor powders were pressed into pellets and then calcined at 1000°C for 6 h and characterized by using analytical techniques. The pellets were then tested for their cell viability and ALP activity using rat osteoblast cells.

EXPERIMENTAL PROCEDURE

In this work, we studied the ef
the osteoblast response as a function
TCP, and 600 ppm, 4100 ppm, and
containing calcium phosphates, Ca(
grade, Fisher Chemicals, Fairlawn, NJ
1.503 for all the samples and two aqu
salt dissolved in deionized water and
For synthesizing 0/ 600/ 4100/ 10100
moles $NH_4H_2PO_4$, a constant amount f
dissolving 0.2932/ 0.2924/ 0.2910/ 0
0.0055 moles of $Zn(NO_3)_2{\cdot}6H_2O$, resp
Ca^{2+} and Zn^{2+} ions was rapidly add
addition, the solution became turbid a
few drops of conc. HNO_3 (15.69 M, I
3±0.1. This clear solution was then sti
NH_4OH (29% NH_3, Merck) causing i
with a pH of 9.2±0.2 at 37°C. This s
precipitates were washed with 4 L v
powders were ground and then press
pressure of 4,500 kg. Thus formed pell

The precursor and calcined sam
(XRD; XDS 2000, Scintag Corp., S
monochromated Cu K_α radiation. X-ray
of 0.03°/minute. Fourier-transformed i
Woburn, MA) analysis was performed
of the precursor particles were evalua
Hitachi Corp., Tokyo, Japan) at 12
calcined pellets was evaluated with a
Corp., Tokyo, Japan) which was used
voltage of 5 kV. Chemical analyses
performed by ICP-AES (Model 61E, T
mg portions of powder samples were d
roughness analyses on calcined pellets
profilometer (Wyko, Tuscon AZ) with
25X. In profilometry, R_a was the aver
highest peak and the lowest valley i
calcined pellets were performed using
GA). For each sample, the number of
along with the standard deviation. Th
Toledo, Columbus, OH) were perform
our powder synthesis route over the ran

7F2 rat osteoblast cells (CRL-1
were grown on 75 cm^2 culture flasks a
(α-MEM) with 2 mM l-glutamine an
deoxyribonucleosides, augmented by 1

EXPERIMENTAL PROCEDURE

In this work, we studied the effect of varying concentrations of Zn in β-TCP to determine the osteoblast response as a function of Zn concentration. The samples prepared were pure β-TCP, and 600 ppm, 4100 ppm, and 10100 ppm Zn-doped β-TCP. For synthesizing these Zn-containing calcium phosphates, $Ca(NO_3)_2{\cdot}4H_2O$, $NH_4H_2PO_4$, and $Zn(NO_3)_2{\cdot}6H_2O$ (Reagent-grade, Fisher Chemicals, Fairlawn, NJ) were used. The (Ca+Zn)/P molar ratio was maintained at 1.503 for all the samples and two aqueous solutions were prepared; one containing a phosphate salt dissolved in deionized water and the second containing Ca and Zn salts dissolved in water. For synthesizing 0/ 600/ 4100/ 10100 ppm Zn-doped β-TCP, the first solution contained 0.1951 moles $NH_4H_2PO_4$, a constant amount for all concentrations. The second solution was prepared by dissolving 0.2932/ 0.2924/ 0.2910/ 0.2877 moles of $Ca(NO_3)_2{\cdot}4H_2O$ and 0 / 0.0008/ 0.0022/ 0.0055 moles of $Zn(NO_3)_2{\cdot}6H_2O$, respectively, in 600 mL water. The latter solution containing Ca^{2+} and Zn^{2+} ions was rapidly added to the phosphate solution. Within few minutes after addition, the solution became turbid and pH was recorded as 4±0.1. To make this solution clear, few drops of conc. HNO_3 (15.69 M, Fisher) were added and the pH of this solution dropped to 3±0.1. This clear solution was then stirred at 37±1°C for 2 h followed by rapid addition of 50 mL NH_4OH (29% NH_3, Merck) causing instantaneous precipitation and a resultant opaque solution with a pH of 9.2±0.2 at 37°C. This suspension was stirred for 1 h and filtered with paper. The precipitates were washed with 4 L water, followed by drying at 90°C overnight. The dried powders were ground and then pressed into pellets using a 1.25 cm diameter steel die and a pressure of 4,500 kg. Thus formed pellets were calcined at 1000°C for 6 hours in air.

The precursor and calcined samples were characterized by using an X-ray diffractometer (XRD; XDS 2000, Scintag Corp., Sunnyvale, CA), operated at 40 kV and 30 mA with monochromated Cu K_α radiation. X-ray data were collected at 2θ values from 25° to 40° at a rate of 0.03°/minute. Fourier-transformed infrared spectroscopy (FTIR; Nicolet 550, Thermo-Nicolet, Woburn, MA) analysis was performed on the precursor and calcined samples. The size and shape of the precursor particles were evaluated by transmission electron microscope (TEM, H7600T, Hitachi Corp., Tokyo, Japan) at 120kV. Surface morphology of the sputter-coated (w/Pt) calcined pellets was evaluated with a scanning electron microscope (FE-SEM; S-4700, Hitachi Corp., Tokyo, Japan) which was used in the secondary electron (SE) mode with an acceleration voltage of 5 kV. Chemical analyses of powder (both precursor and calcined) samples were performed by ICP-AES (Model 61E, Thermo Electron, Madison, WI). For the ICP analyses, 50 mg portions of powder samples were dissolved in 5 mL of concentrated HNO_3 solution. Surface roughness analyses on calcined pellets were performed with a NT-2000 Non-contacting surface profilometer (Wyko, Tuscon AZ) with a 0.164 x 0.215 mm field of view and a magnification of 25X. In profilometry, R_a was the average roughness and R_t was the difference between of the highest peak and the lowest valley in the field of view. The bulk density measurements of calcined pellets were performed using He-pycnometer (AccuPyc 1330, Micromeritics, Norcross, GA). For each sample, the number of purges and runs was 5 and the averages were reported along with the standard deviation. Thermogravimetric analyses (TGA, Model 851e, Mettler-Toledo, Columbus, OH) were performed in an air atmosphere only on the starting chemicals of our powder synthesis route over the range of 30°–1000°C, with a scan rate of 5°C/min.

7F2 rat osteoblast cells (CRL-12557, American Type Culture Collection, Rockville, MD) were grown on 75 cm^2 culture flasks at 37°C and 5% CO_2 in alpha minimum essential medium (α-MEM) with 2 mM l-glutamine and 1 mM sodium pyruvate, without ribonucleosides and deoxyribonucleosides, augmented by 10% FBS. The culture medium was changed every other day until the cells reached a confluence of 90-95%, as determined visually with an inverted microscope. The cells were passaged using trypsin (2.5 g/L)/ EDTA (25mM) solution (Sigma-Aldrich Corp., St. Louis, MO, USA). The obtained cells were then seeded at a concentration of 3500 cell/well on 0.14 cm^3 cylindrical samples for various assays. Cell viability and alkaline phosphatase activity were measured after 72 hours. For statistics, the sample size (*n*) was selected as 16 for all the *in vitro* cell culture tests.

The cell viability assessment was performed using Live/Dead® Viability/Cytotoxicity Kit (L-3224, Molecular Probes, Eugene, OR). The fluorescence values at 494/517 nm for live cells and 528/617 nm for dead cells were recorded. The alkaline phosphatase (ALP) activity was determined using the ALP concentration and the cell extracted protein concentration. The ALP concentration was calculated using Enzymatic Assay of Phosphatase Alkaline Kit (EC 3.1.3.1, Sigma-Aldrich Corp., St. Louis, MO, USA). A working reagent was prepared by first mixing 2.7 ml of Reagent A (1.0 M Diethanolamine Buffer with 0.50 mM Magnesium Chloride) with 0.30 ml of Reagent B (150 mM p-Nitrophenyl Phosphate Solution (pNPP)) and then mixing the mixture with 0.10 ml of cell-containing media. 100 µl of this solution was added to each well and thoroughly mixed and incubated at 37ºC for 30 minutes. Following incubation, the absorbance was recorded at 405 nm with the spectrophotometer at room temperature. The standard curve was obtained by plotting the absorbance measured at 405 nm for certain concentration against the concentration in µg/ml. ALP concentration of each sample was then determined using this standard curve and is expressend as µg-pNP/ml. The cell extracted protein concentration was determined in a two-step procedure, first the protein was extracted using M-PER™ Mammalian Protein Extraction reagent and then this extracted protein was measured using BCA™ Protein Assay Kit. The cell samples were lysed by adding 200 µl of M-PER™ Reagent to each well plate and then shaking for 5 minutes. Lysate was collected and transferred to microcentrifuge tubes, followed by centrifuging at 4000g for 10 minutes to pellet the cell debris. Supernatant was transferred to clean tubes for analyzing the protein concentration. To measure the protein amount, a working reagent (WR) was prepared by mixing 50 parts of BCA™ Reagent A with 1 part of BCA™ Reagent B (50:1, Reagent A:B). 200 µl of the above mentioned WR was added to each well and thoroughly mixed. Following mixing, the well plate was covered and incubated at 37ºC for 30 minutes. The absorbance at 562 nm was measured with the spectrophotometer at room temperature. A standard curve was prepared by plotting the average blank-corrected 562 nm measurement for each BSA standard versus its concentration in µg/ml. Cell extracted protein concentration was then determined by using this standard curve and is expressed as µg/ml. The ALP activity was then calculated as follows; ALP Activity = [(µg pNP)/139] / µg(cell extracted protein) = µmoles pNPP/ µg cell protein. Osteoblast attachment on calcined pellets was examined using SEM (FESEM; S-4700, Hitachi Corp., Tokyo, Japan). Prior to the SEM investigations, cells were fixed by using 3.5% glutaraldehyde. Osteoblasts were dehydrated through sequential washings in 50%, 70%, 95% ethanol solutions and 2 times in 100% ethanol. Samples were then critical point-dried according to the previously published techniques. Samples were sputter-coated with a thin layer of platinum prior to the electron microscope observations performed at 5 kV.

RESULTS AND DISCUSSION

The ICP-AES results (Table 1) showed the Ca, P and Zn levels achieved in the powders after calcinations. Henceforth, the samples will be referred to as Zn-0, Zn-600, Zn-4100, Zn-10100 for 0, 600, 4100, 10100 ppm levels of Zn in β-TCP. It must be noted that there was an increase in Zn levels in going from precursors to 1000°C-calcined samples (results not shown),

Table I ICP-AES results of the calcined samples at 1000°C for 6 h

*Sample**	Ca (%)	P (%)	Ca/P	Zn (*ppm*)
Zn-0	41.21	20.71	1.523	0
Zn-600	42.85	22.14	1.496	600
Zn-4100	36.46	18.94	1.488	4100
Zn-10100	38.92	20.16	1.493	10100

* Samples containing ppm-level Zn in β-TCP

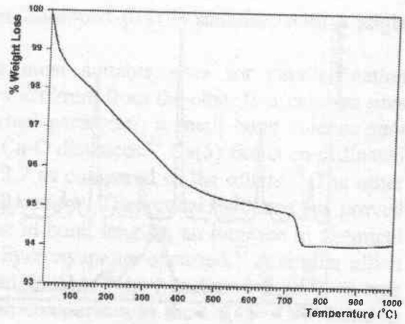

Fig. 1a

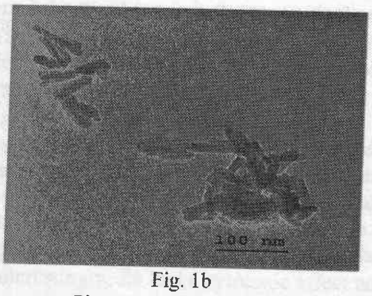

Fig. 1b

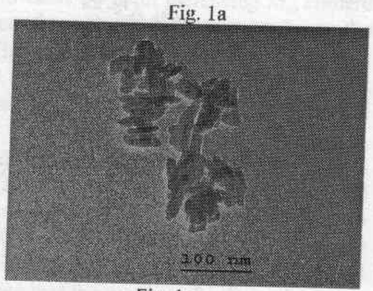

Fig. 1c

Fig. 1 (*a*) TGA trace, (*b*, *c*) TEM micrographs of the precursor powders

which can be attributed to the different forms (i.e., surface/bulk) of Zn present in both sets of samples. Zinc will be more tightly incorporated into the structure after calcination as compared to the surface-adsorbed Zn that might be present in the precursor powders. A total weight loss of around 6% was observed in going from room temperature (RT) to 1000°C (Fig. 1a). The weight loss occurred in two parts, first comprised of a gradual loss from RT to 700°C which meant a loss of some surface adsorbed water, remaining nitrate and/or ammonium ions which were not fully removed during washing. The conversion of hydrogen phosphate ions (HPO_4^{2-}) into $P_2O_7^{4-}$ occurs at the same time, with the evolution of water vapor. Carbonate ions that were present in the FTIR spectra of the precursor material and absent in the calcined samples, constituted the second part. These carbonate ions were removed from the system at around 720°C.

The TEM micrographs (of Figures 1b and 1c) of the precursor material showed that the material was nanocrystalline in nature and consisted of rod-shaped crystals of about 50 nm-length and 15 nm-thickness. Due to the high concentration of the powders in solution, these crystals tended to form agglomerates. These agglomerates were believed to be soft agglomerates as these were later on pressed to form a pellet. Although the sample preparation routes of this study differed significantly from that of Bouyer *et al.*,[43] the particle shape and size was quite similar.

XRD patterns of the pure and Zn-doped precursor powders and sintered samples were shown in Figure 2a. The nanorods or nanoneedles of the precursor powder yielded an XRD pattern similar to that of poorly-crystallized apatitic calcium phosphate. Sintered samples (both

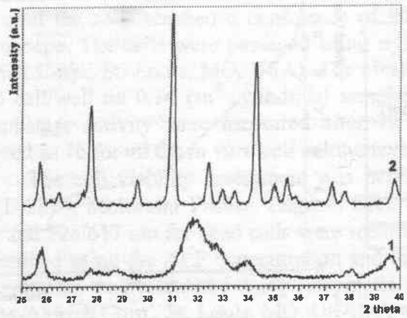

Fig. 2a

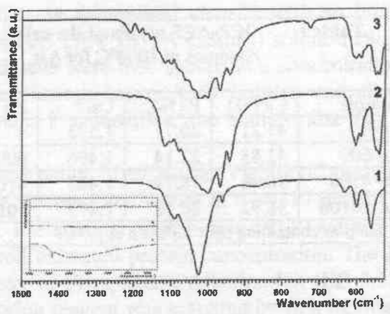

Fig. 2b

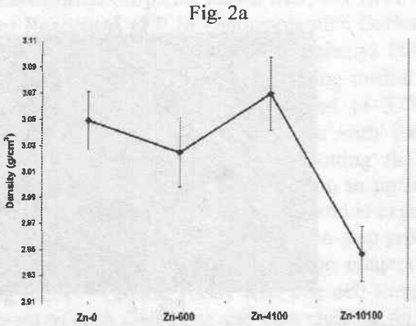

Fig. 2c

Table II Surface profilometry on sintered samples

Sample	R_a*	R_t**
Zn-0	0.52 ± 0.07	13.41 ± 1.76
Zn-600	0.53 ± 0.05	7.69 ± 1.50
Zn-4100	0.35 ± 0.03	4.33 ± 0.89
Zn-10100	0.52 ± 0.02	9.57 ± 1.49

* *Average roughness*
** *Maximum height minus minimum height in the field of view*

Fig. 2 (*a*) XRD trace, and (*b*) FTIR trace of the precursor powder (1), sintered sample (2), and Fluka TCP powder, (*c*) pycnometric results (bulk densities) of sintered pellets

pure and Zn-doped) resulted in the characteristic β-TCP XRD patterns. The FTIR spectra (Fig. 2b) confirmed the X-ray analyses, where a band at 3571 cm^{-1} was observed (see inset in Fig. 2b) substantiating the presence of apatitic phase in the precursors. The OH^- band in the sintered samples was absent, indicating the conversion to β-TCP. The characteristic IR spectrum for the commercial β-TCP powders (i.e., Fluka, Inc.) was added as trace 3 to Fig. 2b. The IR bands of trace 2 and trace 3 of this chart match closely. The precursors after pelletization and calcination resulted in highly dense pellets, the bulk density values reported in Figure 2c. The bulk density of β-TCP is 3.15 gm/cc, which confirms the attainment of more than 95% density in Zn-doped β-TCP. The maximum densification was observed in the sample of Zn-4100. Interestingly, this sample (Zn-4100) exhibited the lowest average surface roughness among all the samples. Average surface roughness and highest-to-lowest peak values are reported in Table 2, which showed the lowest values for Zn-4100, thus the sample with the smoothest surface. This effect was quite evident from the SEM micrographs of sintered pellets (shown in Figure 3), where a decrease in grain size was observed when Zn levels were either increased or decreased from 4100 ppm. The grain sizes were ranging from 350 nm to 2 μm for Zn-4100 and ranged from a 100 nm to < 1μm for the rest of Zn-dopant levels. This grain growth as a function of substitution of divalent ions into β-TCP was also observed by Yoshida *et al.*[44] They reported an increase in the grain size until 11.5 mol% Mg^{2+} ion substitution and observed a decrease in the grain size thereafter. This case resembles our study in which instead of Mg^{2+} we used Zn^{2+} and that the

maximum grain growth was observe
decrease in grain sizes thereafter.

In β-TCP, Ca(4) and Ca(5)
substitution.[45] The site Ca(4) was confi
with a lower occupancy factor, highe
(BVS), small co-ordination number (C
with six oxygen atoms and has the hi
cation sites do not offer a suitable geo
that when Zn^{2+} ion substitution took p
stability and a deformation of the cryst
was also observed when Mg^{2+} ions
observed that the Mg(4)•••O(9) bond
pure β-TCP.[45, 48] The O•••Mg(5)•••O b
confirmed the trend towards the more
similarity in the lattice constants of Z
cationic sites is expected from both t
substitution in β-TCP will lead to sho
stability.

Mouse osteoblast cells (7F2)
of the number of attached cells and alk
4b. The initial number of cells seeded
days the number of live cells on Zn-0
doped pellets had greater number of li
level. Interestingly, Zn had a cytotoxic

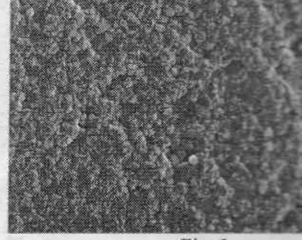

Fig. 3a

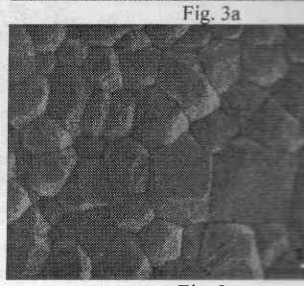

Fig. 3c

Fig. 3 SEM micrographs of (*a*) pure

maximum grain growth was observed at 4100 ppm Zn-doped β-TCP samples, with a slight decrease in grain sizes thereafter.

In β-TCP, Ca(4) and Ca(5) sites are the most suitable sites for smaller cation substitution.[45] The site Ca(4) was confirmed to be very different from the other four calcium sites with a lower occupancy factor, higher isotropic thermal parameter, a small bond valence sum (BVS), small co-ordination number (CN) and longer Ca-O distances.[46] Ca(5) site is co-ordinated with six oxygen atoms and has the highest BVS of 2.7 as compared to the others.[46] The other cation sites do not offer a suitable geometry for small cations. Theoretical evidence has proved that when Zn^{2+} ion substitution took place, a decrease in bond lengths, an increase in chemical stability and a deformation of the crystal structure of hydroxyapatite occurred.[47] A similar effect was also observed when Mg^{2+} ions were substituted in HA.[47] In Mg-doped β-TCP, it was observed that the Mg(4)•••O(9) bond was shortened in comparison to the Ca(4)•••O(9) bond in pure β-TCP.[45, 48] The O•••Mg(5)•••O bonds approached towards 90° with increasing Mg content confirmed the trend towards the more ideal octahedral configuration.[45, 48] Moreover, due to the similarity in the lattice constants of Zn and Mg, a similar preferential distribution in different cationic sites is expected from both the theoretical and experimental studies.[8] Therefore, zinc substitution in β-TCP will lead to shortening of the bond lengths and an increase in chemical stability.

Mouse osteoblast cells (7F2) cultured on calcined pellets exhibited differences in terms of the number of attached cells and alkaline phosphatase activity, as presented in Figures 4a and 4b. The initial number of cells seeded onto the calcined pellets was 3500 cells/pellet and after 3 days the number of live cells on Zn-0 sample increased to about 15000 cells. All the other Zn-doped pellets had greater number of live cells, with the highest being at 4100 ppm Zn-dopant level. Interestingly, Zn had a cytotoxic effect and it was seen that the number of cell death was

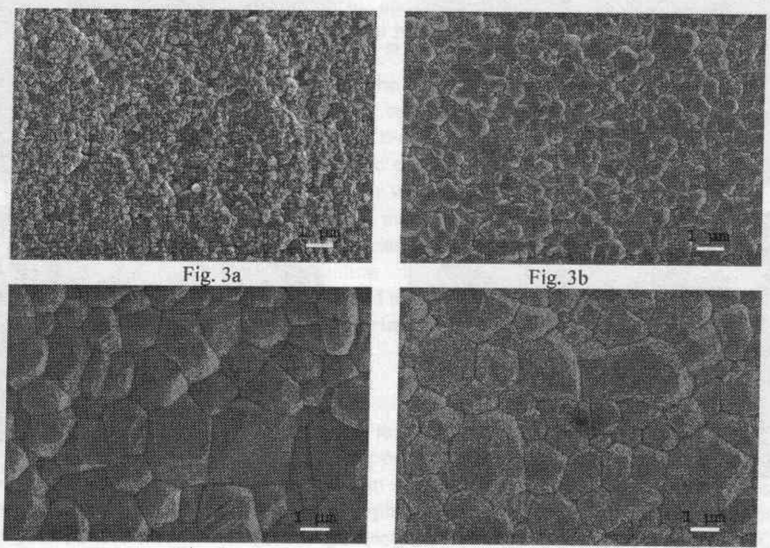

Fig. 3a Fig. 3b Fig. 3c Fig. 3d

Fig. 3 SEM micrographs of (*a*) pure β-TCP, (*b*) Zn-600, (*c*) Zn-4100, and (*d*) Zn-10100 pellet maximum on the pellets which contained the highest amount of Zn-level in this study, that was, Zn-10100. The % dead cells were calculated for all the samples, and a descending trend was observed with Zn-10100 sample showing the highest % dead cells at around 21% and the least was observed for pure-TCP sample (4%). Therefore, zinc stimulated the growth of osteoblasts and we observed that the osteoblasts multiplied by ten-fold within 3 days in Zn-doped samples, whereas the multiplication rate was only 5-fold in Zn-0 (pure -TCP). The osteoblast cells require the presence of certain ions and proteins (i.e., nutrients) in the media for growth and propagation.[49] We may speculate that at the very beginning of the cell culture tests, the amount

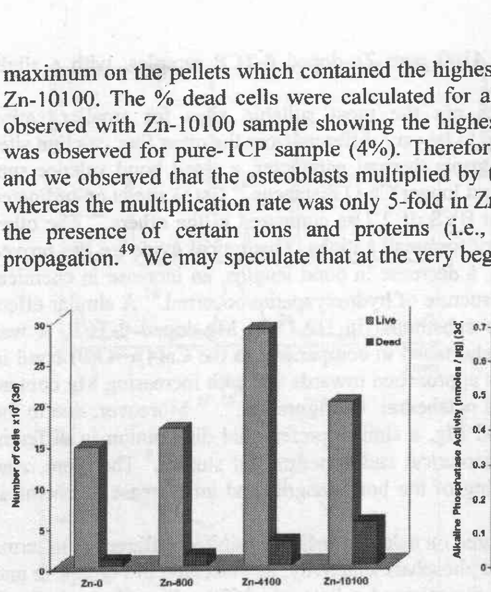

Fig. 4a

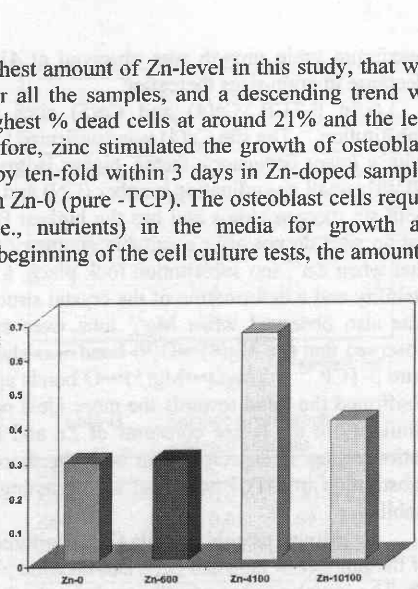

Fig. 4b

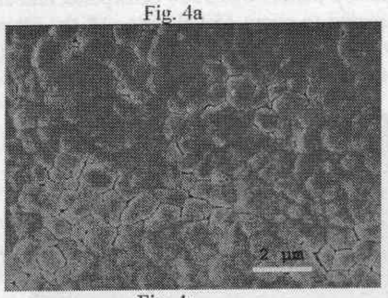

Fig. 4c

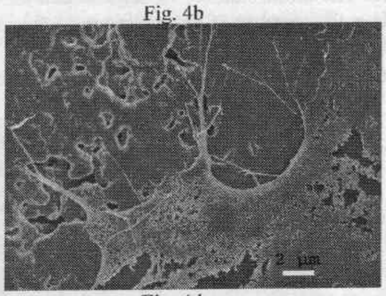

Fig. 4d

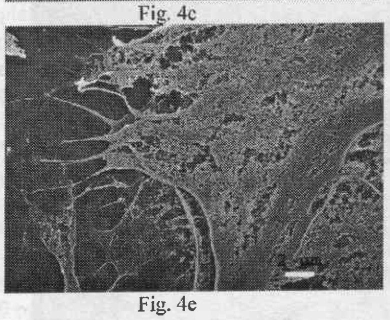

Fig. 4e

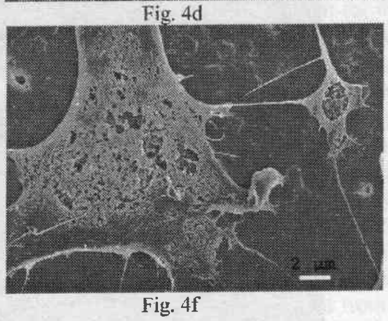

Fig. 4f

Fig. 4 (*a*) Cell viability (*live/dead*), (*b*) ALP activity for Zn-0, Zn-600, Zn-4100 and Zn-10100; SEM micrographs of osteoblasts on the surface of (*c*) pure β-TCP (*d*) Zn-600, (*e*) Zn-4100, and (*f*) Zn-10100 pellet

of ions in the media was sufficient w
replenished during the 3- day cultu
concentration of the essential ions an
was also found to yield the highest v
decrease in both the ALP activity and
levels from 4100 ppm. Osteoblast atta
was monitored by FESEM, and given
surfaces of all the samples tested here
behavior. Cells were able to easily
sintered pellets. In Zn-0 pellet (pure
associated with the pellet, as they for
visible (Fig. 4c). In Zn-doped pellets,
filopodia extending onto the pellet sur
in these samples as compared to the f
Briefly, the extent of cell spreading wa
Factors like surface roughness
interactions.[51, 52] Many researchers cl
spreading should be observed.[52, 53]
studies demonstrated that greatest o
rougher surfaces with more irregular
al.[50] to evaluate the material-cell inter
highest on Thermanox plastic as con
study, it was shown that proliferation
osteoblasts on the composite calcium
40% when compared to Thermanox
These suggest that the *in vitro* observ
better *in vivo* bone integration for that
terms of osteoblast spreading and ac
(roughest surface in this study) while
pellet with the smoothest surface, that
doping apparently led to the onset of
higher (Fig. 4b) and the surfaces of the
In consequence, these results s
activity were the factors which are mo
spreading alone, in evaluating the in
question. Evidence presented here larg
and partially satisfied our quest for th
TCP to improve the osteoblast respons

CONCLUSIONS

A wet chemical method was de
and Zn-doped β-TCP (0, 600, 4100 an
the Zn-dopant levels achieved in all th
technique like ICP, for the first tim
consisting of nanorods or nanoneedle
relatively low temperature of 1000°C.

of ions in the media was sufficient which helped the cells to multiply. Since the media was not replenished during the 3- day culture tests, cell death was observed due to a decreased concentration of the essential ions and proteins in the media. The alkaline phosphatase activity was also found to yield the highest values for Zn-level of 4100 ppm in the sintered pellets. A decrease in both the ALP activity and live cells was observed with an increase or decrease in Zn-levels from 4100 ppm. Osteoblast attachment and proliferation on the surfaces of sintered pellets was monitored by FESEM, and given in Figures 4c through 4f. Osteoblasts were attached to the surfaces of all the samples tested here, however, the osteoblast proliferation showed a significant behavior. Cells were able to easily differentiate between the chemical compositions of the sintered pellets. In Zn-0 pellet (pure β-TCP), the osteoblast cell was observed to be closely associated with the pellet, as they formed a translucent layer through which the grains were still visible (Fig. 4c). In Zn-doped pellets, osteoblasts appeared to be more elongated with numerous filopodia extending onto the pellet surfaces. The cells were also slightly raised above the surface in these samples as compared to the flattened morphology observed for the pure β-TCP pellets. Briefly, the extent of cell spreading was the highest in Zn-0 (pure β-TCP) pellets.

Factors like surface roughness and composition of a surface influence the material-cell interactions.[51, 52] Many researchers claimed that on smooth surfaces, better cell adhesion and spreading should be observed.[52, 53] However, there are discrepancies in literature and some studies demonstrated that greatest osteoblast attachment and proliferation was observed on rougher surfaces with more irregular topographies.[54, 55] An SEM study performed by Baxter *et al.*[50] to evaluate the material-cell interaction concluded that the spreading of the osteoblasts was highest on Thermanox plastic as compared to that of HA substrates. Interestingly, in another study, it was shown that proliferation numbers and alkaline phosphatase (ALP) activities of the osteoblasts on the composite calcium phosphate coatings were improved by approximately 30-40% when compared to Thermanox control, and were comparable to the pure HA coating.[56] These suggest that the *in vitro* observation of a high cell spreading would not necessarily mean better *in vivo* bone integration for that material.[50] In our study, we observed a mixed response in terms of osteoblast spreading and activity. The best spreading was observed on pure β-TCP (roughest surface in this study) while the best osteoblast activity was observed on a Zn-doped pellet with the smoothest surface, that is, at a Zn-dopant level of 4100 ppm. Higher levels of Zn-doping apparently led to the onset of cytotoxic effects (Fig. 4a), but still the ALP activity was higher (Fig. 4b) and the surfaces of those pellets were coarser than those of pure β-TCP.

In consequence, these results suggested that material composition, cell viability and ALP activity were the factors which are more important than the surface roughness and extent of cell spreading alone, in evaluating the interaction of osteoblast cells with the biomaterial under question. Evidence presented here largely added to the previous work performed by Ito *et al.*,[30-42] and partially satisfied our quest for the determination of the appropriate Zn dopant level in β-TCP to improve the osteoblast response.

CONCLUSIONS

A wet chemical method was developed and successfully used for the synthesis of β-TCP and Zn-doped β-TCP (0, 600, 4100 and 10100 ppm Zn), after carefully and extensively checking the Zn-dopant levels achieved in all the resultant samples by using an accurate chemical analysis technique like ICP, for the first time. Zn-doping, as well as the use of precursor powders consisting of nanorods or nanoneedles, significantly improved the densification of β-TCP at a relatively low temperature of 1000°C. Zn-doping caused a slight grain growth, in comparison to pure β-TCP, up to a certain dopant level, which then decreased or leveled off with further increase in the dopant level. The highest number of live rat osteoblast cells was observed for the 4100 ppm Zn-doped β-TCP pellet. This proved that even the ppm level presence of Zn (solely originating from the sintered pellet samples themselves) in a cell culture medium has an undeniable effect in stimulating the multiplication and proliferation of osteoblasts. The highest alkaline phosphatase activity was again encountered for the same Zn-4100 sample. Doping of sintered β-TCP porous blocks, sponges or granules, which are already in clinical use as bone substitutes, with Zn over the range of 3000 to 4000 ppm may cause a significant increase in the osteoblast response and proliferation on such samples. This has been the most critical and technologically important conclusion of this study.

ACKNOWLEDGEMENTS

The work is partially supported by NSF 0522057.

REFERENCES

[1] J.C. Heughebaert, and G. Bonel, "Composition, stuctures and properties of calcium phosphates of biological interest," In: Christel P, Meunier A, Lee AJC (eds); *Biological and Biomechanical Performance of Biomaterials* (Elsevier Science Publishers), 9-14 (1986).

[2] C.E. Rawlings, J.A. Persing, and J.M. Tew, "Modern bone substitutes with emphasis on calcium-phosphate ceramics and osteoinductors," *Neurosurgery*, **33**, 935-8 (1993).

[3] A. C. Tas, "Participation of calcium phosphate bone substitutes in the bone remodeling process: Influence of materials chemistry and porosity," *Key Eng. Mat.*, **264-268**, 1969-72 (2004).

[4] A. Bigi, E. Foresti, M. Gandolfi, and N. Roveri, "Inhibiting effect of zinc on hydroxylapatite crystallization," *J. Inorg. Biochem.*, **58**, 49-58 (1995).

[5] R. Tang, M. Hass, W. Wu, S. Gulde, and G. H. Nancollas, "Constant Composition of Mixed Phases II Selective Dissolution of Calcium Phosphates," *J. Colloid. Interf. Sci.*, **260**, 379-84 (2003).

[6] A. Ito, H. Kawamura, S. Miyakawa, P. Layrolle, N. Kanzaki, G. Treboux, K. Onuma, and S. Tsutsumi, "Resorbability and solubility of zinc-containing tricalcium phosphate," *J. Biomed. Mater. Res.*, **60**, 224-31 (2002).

[7] I. Manjubala, and T.S.S. Kumar, "Preparation of biphasic calcium phosphate doped with magnesium fluoride for osteoporotic applications," *J. Mater. Sci. Lett.*, **20**, 1225-7 (2001).

[8] A. Bigi, E. Foresti, M. Gandolfi, M. Gazzano, and N. Roveri, "Isomorphous substitutions in beta-tricalcium phosphate: The different effects of zinc and strontium," *J. Inorg. Biochem.*, **66**, 259-65 (1997).

[9] R. Tang, W. Wu, M. Haas, and G.H. Nancollas, "Kinetics of Dissolution of b-Tricalcium Phosphate," *Langmuir*, **17**, 3480-5 (2001).

[10] W. Wu, R. Tang, M. Haas, and G.H. Nancollas, "Constant Composition Dissolution Kinetics of Mixed Phases I. Synthetic Calcium Phosphates," *J. Coll. Interf. Sci.*, **244**, 347-52 (2001).

[11] E.R. Kreidler, and F.A. Hummel, "Phase equilibria in the system $Ca_3(PO_4)_2$ - $Zn_3(PO_4)_2$," *Inorg. Chem.*, **6**, 524-8 (1967).

[12] A.S. Prasad, "Clinical, endocrinological and biochemical effects of zinc-deficiency," *Clin. Endocrinol. Meta.*, **14**, 567-89 (1985).

[13] M. Hambidge, "Human zinc deficiency," *J. Nutr.*, **130**, 1344S-49S (2000).

[14] M. Yamaguchi, and R. Yamaguchi, "Action of zinc on bone metabolism in rats - increases in alkaline-phosphatase activity and DNA content," *Biochem. Pharmacol.*, **35,** 773–7 (1986).

[15] S.L. Hall, H.P. Dimai, and J.R. Farley, "Effects of zinc on human skeletal alkaline phosphatase activity in vitro," *Calcif. Tiss. Int.*, **64,** 163-72 (1999).

[16] D. Hatakeyama, O. Kozawa, T. Otsuka, T. Shibata, and T. Uematsu, "Zinc suppresses IL-6 synthesis by prostaglandin F-2 alpha in osteoblasts: Inhibition of phospholipase C and phospholipase D," *J. Cell. Biochem.*, **85,** 621-8 (2002).

[17] S.K. Lim, Y.J. Won, H.C. Lee, K. Huh, and Y.S. Park, "A PCR analysis of ER alpha and ER beta mRNA abundance in rats and the effect of ovariectomy," *J. Bone Miner. Res.*, **14,** 1189-96 (1999).

[18] E. Sugimoto and M. Yamaguchi, "Stimulatory effect of daidzein in osteoblastic MC3T3-E1 cells," *Biochem. Pharmacol.*, **59,** 471-5 (2000).

[19] K. Ishida, N. Sawada, and M. Yamaguchi, "Expression of albumin in bone tissues and osteoblastic cells: Involvement of hormonal regulation," *Int. J. Mol. Sci.*, **14,** 891-5 (2004).

[20] M. Yamaguchi, S. Kishi, and M. Hashizume, "Effect of zinc-chelating dipeptides on osteoblastic MC3T3-E1 cells - activation of aminoacyl-transfer-rna synthetase," *Peptides*, **15,** 1367-71 (1994).

[21] K. Nakashima, X. Zhou, G. Kunkel, Z. Zhang, J. M. Deng, R. R. Behringer, and B. de Crombrugghe, "The novel zinc finger-containing transcription factor Osterix is required for osteoblast differentiation and bone formation," *Cell*, **108,** 17-29 (2002).

[22] L.S. Hurley, J. Gowan, and G. Milhaund , "Calcium metabolism in. manganese deficient and zinc deficient rats," *P. Soc. Exp. Biol. Med.*, **130,** 856-60 (1969).

[23] G. Oner, B Bhaumick, and R.M. Bala, "Effect of zinc deficiency on serum somatomedin levels and skeletal growth in young rats," *Endocrinology*, **114,** 1860-3 (1984).

[24] M. Hertzberg, J. Foldes, R. Steinberg, and J. Menczel, "Zinc excretion in osteoporotic women.," *J. Bone Miner. Res.*, **5,** 251-7 (1990).

[25] P.J. Fraker, "Roles for cell death in zinc deficiency," *J. Nutr.*, **135,** 359-62 (2005).

[26] R.J.P. Williams, "Zinc: what is its role in biology?," *Endeavour*, **8,** 65-70 (1984).

[27] T.A. Fuierer, M. LoRe, S.A. Puckett, and G.H. Nancollas, "A mineralization adsorption and mobility study of hydroxyapatite surfaces in the presence of zinc and magnesium ions," *Langmuir*, **10,** 4721-5 (1994).

[28] R.Z. LeGeros, *Caries Res.* **31,** 434 (1997).

[29] R.Z. LeGeros, C.B. Bleiwas, M. Retino, R. Rohanizadeh, and J.P. LeGeros, "Zinc effect on the in vitro formation of calcium phosphates: Relevance to clinical inhibition of calculus formation," *Am. J. Dent.*, **12,** 65-71 (1999).

[30] N. Kanzaki, K. Onuma, G. Treboux, S. Tsutsumi, and A. Ito, "Inhibitory effect of magnesium and zinc on crystallization kinetics of hydroxyapatite (0001) face," *J. Phys. Chem. B.*, **104,** 4189-94 (2000).

[31] A. Ito, K. Ojima, H. Naito, N. Ichinose, and T. Tatseishi, "Preparation, solubility, and cytocompatibility of zinc-releasing calcium phosphate ceramics," *J. Biomed. Mater. Res.*, **50,** 178-83 (2000).

[32] H. Kawamura, A. Ito, S. Miyakawa, P. Layrolle, K. Ojima, N. Ichinose, and T. Tateishi, "Stimulatory effect of zinc-releasing calcium phosphate implant on bone formation in rabbit femora," *J. Biomed. Mater. Res.*, **50,** 184-90 (2000).

[33] M. Otsuka, S. Marunaka, Y. Matsuda, A. Ito, P. Layrolle, H. Naito, and N. Ichinose, "Calcium level-responsive in-vitro zinc release from zinc containing tricalcium phosphate (ZnTCP)," *J. Biomed. Mater. Res.*, **52**, 819-24 (2000).

[34] N. Kanzaki, K. Onuma, G. Treboux, S. Tsutsumi, and A. Ito, "Effect of impurity on two-dimensional nucleation kinetics: Case studies of magnesium and zinc on hydroxyapatite (0001) face," *J. Phys. Chem. B.*, **105**, 1991-4 (2001).

[35] A. Ito, H. Kawamura, M. Otsuka, M. Ikeuchi, H. Ohgushi, K. Ishikawa, K. Onuma, N. Kanzaki, Y. Sogo, and N. Ichinose, "Zinc-releasing calcium phosphate for stimulating bone formation ," *Mat. Sci. Eng. C-Bio. S.*, **22**, 21-5 (2002).

[36] K. Ishikawa, Y. Miyamoto, T. Yuasa, A. Ito, M. Nagayama, and K. Suzuki, "Fabrication of Zn containing apatite cement and its initial evaluation using human osteoblastic cells," *Biomaterials*, **23**, 423-8 (2002).

[37] Y. Sogo, T. Sakurai, K. Onuma, and A. Ito, "The most appropriate (Ca plus Zn)/P molar ratio to minimize the zinc content of ZnTCP/HAP ceramic used in the promotion of bone formation," *J. Biomed. Mater. Res.*, **62**, 457-63 (2002).

[38] H. Kawamura, A. Ito, T. Muramatsu, S. Miyakawa, N. Ochiai, and T. Tateishi, "Long-term implantation of zinc-releasing calcium phosphate ceramics in rabbit femora," *J. Biomed. Mater. Res.*, **65A**, 468-74 (2003).

[39] M. Ikeuchi, A. Ito, Y. Dohi, H. Ohgushi, H. Shimaoka, K. Yonemasu, and T. Tateishi, "Osteogenic differentiation of cultured rat and human bone marrow cells on the surface of zinc-releasing calcium phosphate ceramics," *J. Biomed. Mater. Res.*, **67A**, 1115-22 (2003).

[40] Y. Sogo, A. Ito, M. Kamo, T. Sakurai, K. Onuma, N. Ichinose, M. Otsuka, and R.Z. LeGeros, "Hydrolysis and cytocompatibility of zinc-containing alpha-tricalcium phosphate powder ," *Mat. Sci. Eng. C-Bio. S.*, **24**, 709-15 (2004).

[41] M. Otsuka, Y. Ohshita, S. Marunaka, Y. Matsuda, A. Ito, N. Ichinose, K. Otsuka, and W.I. Higuchi, "Effect of controlled zinc release on bone mineral density from injectable Zn-containing beta-tricalcium phosphate suspension in zinc-deficient diseased rats," *J. Biomed. Mater. Res.*, **69A**, 552-60 (2004).

[42] A. Ito, M. Otsuka, H. Kawamura, M. Ikeuchi, H. Ohgushi, Y. Sogo, and N. Ichinose, "Zinc-containing tricalcium phosphate and related materials for promoting bone formation," *Curr. Appl. Phys.*, **5**, 402-6 (2005).

[43] E. Bouyer, F. Gitzhofer, and M. I. Boulos, "Morphological study of hydroxyapatite nanocrystal suspension," *J. Mater. Sci.-Mater. M.*, **11**, 523-31 (2000).

[44] K. Yoshida, N. Kondo, H. Kita, M. Mitamura, K. Hashimoto, and Y. Toda, "Effect of Substitutional monovalent and divalent metal ions on mechanical properties of β-tricalcium phosphate," *J. Am. Ceram. Soc.*, **88**, 2315-2318 (2005).

[45] X. Wei, and M. Akinc, "Resorption rate tunable bioceramic: Si&Zn-modified tircalcium phosphate," *Advances in Bioceramics and Biocomposites*, **26**, 129-36 (2005).

[46] M. Yashima, A. Sakai, T. Kamiyama, and A. Hoshikawa, "Crystal structure analysis of β-tricalcium phosphate $Ca_3(PO_4)_2$ by neutron powder diffraction," *J. Solid State Chem.*, **175**, 272-7 (2003).

[47] I. Gutowska, Z. Machoy, and B. Machalinski, "The role of bivalent metals in hydroxyapatite structures as revealed by molecular modeling with the HyperChem software," *J. Biomed. Mater. Res.*, **75A**, 788-93 (2005).

[48] L.W. Schroeder, B. Dickens, a
Mg as a stabilizing impurity in β-trica
tricalcium phosphate," *J.Solid State Che*

[49] http://www.atcc.org/comm
12557.

[50] L.C. Baxter, V. Frauchiger, M
and osteoblast adhesion and morpholog
Materials, **4**, 1-17 (2002).

[51] Z. Schwartz, and B.D. Boyan,
interface," *J.Cell. Biochem.*, **56**, 340-7 (1

[52] K. Mustafa, J. Wroblewski,
titanium surfaces blasted with TiO2 par
morphology of cells derived from hum
(2000).

[53] F.B. Bagambisa, H.F. Kappe
events at the implant interface," *J. Crani*

[54] I. Degasne, M.F. Basle, V. De
D. Chappard, "Effects of roughness, fi
proliferation of human osteoblast-like ce
499-507 (1999).

[55] Z. Schwartz, C.H. Lohmann, J.
"Implant surface characteristics modul
lineage," *Adv. Dent. Res.*, **13**, 38-48 (199

[56] H.W. Kim, G. Georgiou,
phosphates and glass composite coa
Biomaterials, **25**, 4203-13 (2004).

[48] L.W. Schroeder, B. Dickens, and W.E. Brown, "Crystallographic studies of the role of Mg as a stabilizing impurity in β-tricalcium phosphate: II Refinement of Mg-containing β-tricalcium phosphate," *J.Solid State Chem.*, **22,** 253-62 (1977).
[49] http://www.atcc.org/common/catalog/numSearch/numResults.cfm?atccNum=CRL-12557.
[50] L.C. Baxter, V. Frauchiger, M. Textor, I. ap Gwynn, and R.G. Richards, "Fibroblast and osteoblast adhesion and morphology on calcium phosphate surfaces," *European Cells and Materials*, **4**, 1-17 (2002).
[51] Z. Schwartz, and B.D. Boyan, "Underlying mechanisms of the bone-biomaterial interface," *J.Cell. Biochem.*, **56**, 340-7 (1994).
[52] K. Mustafa, J. Wroblewski, K. Hultenby, L.B. Silva, and K. Arvidson, "Effects of titanium surfaces blasted with TiO2 particles on the initial attachment and altered cytoskeletal morphology of cells derived from huma madibular bone," *Clin. Oral. Impl. Res.*, **11,** 116-28 (2000).
[53] F.B. Bagambisa, H.F. Kappert, and W. Schilli, "Cellular and molecular biological events at the implant interface," *J. Cranio. Maxill. Surg.*, **22**, 12-7 (1994).
[54] I. Degasne, M.F. Basle, V. Demais, G. Hure, M. Lesourd, B. Grolleau, L. Mercier, and D. Chappard, "Effects of roughness, fibronectin and vitronectin on attachment, spreading and proliferation of human osteoblast-like cells (Saos-2) on titanium surfaces," *Calcif. Tissue Int.*, **64**, 499-507 (1999).
[55] Z. Schwartz, C.H. Lohmann, J. Oefinger, L.F. Bonewald, D.D. Dean, and B.D. Boyan, "Implant surface characteristics modulate differential behaviour of cells in the osteoblast lineage," *Adv. Dent. Res.*, **13,** 38-48 (1999).
[56] H.W. Kim, G. Georgiou, J.C. Knowles, Y.H. Koh, and H.E. Kim, "Calcium phosphates and glass composite coatings on zirconia for enhanced biocompatibility," *Biomaterials*, **25**, 4203-13 (2004).

WILEY

Advances in Bioceramics and Biocomposites II

Edited by

Mineo Mizuno

Volume editors

Andrew Wereszczak

Edgar Lara-Curzio

The American Ceramic Society

Visit www.wiley.com/go/acers

WILEY
wiley.com

BICENTENNIAL
1807
WILEY
2007
BICENTENNIAL

ISBN 0-470-08056-6
90000
9 780470 080566